# Site-specific Magnetism in $Nd_2Fe_{14}B$ Single Crystal

D. Haskel,[1] J. Lang,[1] Z. Islam,[1] G. Srajer,[1] J. Cross,[2] P. Canfield[3]
[1] Advanced Photon Source (APS), Argonne National Laboratory, Argonne, IL, U.S.A.
[2] Physics Department, University of Washington, Seattle, WA, U.S.A.
[3] Physics Department, Iowa State University, and Ames Laboratory, Ames, IA, U.S.A.

## Introduction

The ability of x-ray based techniques to separate magnetic contributions from different elements in a sample (element-specificity) has proven to be very valuable in studies of complex magnetic materials. In the case of x-ray magnetic circular dichroism (XMCD), this separation is achieved by tuning the x-ray energy to element-specific electron excitations whose response to circularly polarized (CP) x-rays of opposite helicities can be used to extract magnetic information from the excited element only [1].

Complex materials, however, feature elements of the same species in inequivalent crystal sites. These sites are dictated by the symmetry group of the crystal and exhibit unique crystalline environments. The ability to separate the magnetic signals from these sites is important in, for example, understanding the atomic origins of magneto-crystalline anisotropy (MCA), which is strongly tied to the local crystalline environment through crystal field effects. The XMCD technique, however, averages over inequivalent crystal sites of the same species. In the case of $Nd_2Fe_{14}B$, Nd magnetic moments dominate the MCA over Fe moments due to their large 4f orbital moments [2]. Spin-dependent density functional theoretical calculations (local spin density approximation or LSDA) show that the crystal fields at the two Nd inequivalent crystal sites are markedly different [3], leading to the expectation that their intrinsic MCAs will differ as well. The magnetic signals from these inequivalent sites could not as yet be separated.

## Methods and Materials

The x-ray measurements were performed at undulator beamline station 4-ID-D at the APS. Undulator radiation was monochromatized with a Si(111) double-crystal monochromator, and its polarization was converted from linear to circular with a diamond (111) phase retarder operated in Bragg transmission geometry. The single crystal was placed in the field of an electromagnet (≈6 kOe) for room-temperature measurements or a permanent magnet (≈2.4 kOe) for low-temperature measurements. The crystal was aligned with its [110] direction oriented along the scattering vector, and the magnetic field was applied along the [001] direction, which was parallel to the sample surface and in the scattering plane. A closed-cycle He refrigerator mounted in the $\phi$ circle of a diffractometer was used for the low-temperature measurements. The resonant diffraction measurements were carried out through the Nd $L_2$ resonance ($2p_{1/2}$ excitation at 6.722 keV) by switching the helicity of the incident CP x-rays at each energy point while maintaining a given diffraction condition (fixed Q) at all energies. No polarization analysis of the scattered radiation was performed. XMCD measurements were simultaneously performed by measuring the difference in Nd $L_\beta$ fluorescence intensity for opposite x-ray helicities at each energy point through the Nd $L_2$ absorption edge by using energy-dispersive Ge solid-state detectors.

## Results and Discussion

Figure 1 shows resonant diffraction data for (110) and (220) Bragg peaks through the Nd $L_2$ resonance. These reflections alternately probe 4g and 4f Nd crystal sites,

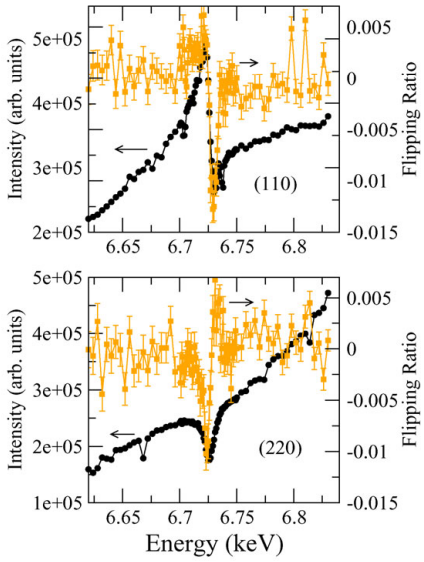


*FIG. 1. Resonant charge scattered intensity (dark circles) and charge-magnetic-interference scattered intensity (light squares) obtained by adding and subtracting scattered intensities for opposite x-ray helicities. The x-ray helicity is switched at each energy point while the diffraction condition is maintained. Data is for T = 300K with an H = 6 kOe applied field along the [001] easy axis direction, contained in the scattering plane.*

respectively. The resonant-charge scattering is obtained from the sum of scattered intensities for opposite x-ray helicities, $(I^+ + I^-)$, while the difference in scattered intensities $(I^+ - I^-)$ is due to charge-magnetic-interference scattering. This interference scattering is proportional to the magnitude of the magnetic moment and also contains information about the moment's direction relative to the x-ray polarization vectors [4].

Element- and site-specific hysteresis loops, shown in Fig. 2, were monitored under the different diffraction conditions by recording changes in the flipping ratio as a function of the applied field while maintaining the diffraction condition at selected energies that optimized charge-magnetic interference signals. The inequivalent sites clearly display different magnetization reversals, with the 4g sites switching at a larger reversed applied field than the 4f sites. This occurs probably because the different crystal fields at the inequivalent sites result in different MCA constants and a larger energy barrier for the switching of the 4g sites. For the two reflections discussed here, the polarization dependence of the charge-magnetic interference signal yield a signal near zero when the magnetization is along the [110] direction. This implies that at a reversed applied field of ≈–500 Oe, the magnetizations of Nd 4g and 4f sites nearly orthogonal to one another (the 4g site is still magnetized along the [001] direction at this field). The ferromagnetic Nd-Nd magnetic coupling in this material is indirect, through exchange interactions with the surrounding Fe ions. The results imply that MCA strongly affects the magnetization reversal in this material — a reversal that includes largely noncollinear configurations of Nd moments. It is likely that Fe moments, which mediate the Nd-Nd ferromagnetic coupling, participate in this unconventional mechanism of reversal as well.

The response to the spin-reorientation transition (SRT) of the magnetic moments of inequivalent Nd sites is obtained by measuring the T-dependent flipping ratio for the different diffraction conditions. Since $Nd_2Fe_{14}B$ is a high-temperature ferromagnet with a $T_c$ of ≈585K, the magnitude of the Nd moments is practically constant below room temperature. Changes in measured intensities are due to the angular dependence of the charge-magnetic-interference scattering as the magnetization reorients from a [001] easy axis toward the basal plane. This known angular dependence was used to extract the rotation of the Nd moments at each site through the SRT, as shown in Fig. 3. The results show that the final spin-reoriented configuration displays significant noncollinearity of the inequivalent Nd sublattices, by about 10° to 15°. The larger error bars at the small canting angles are due to the relative insensitivity of the charge-

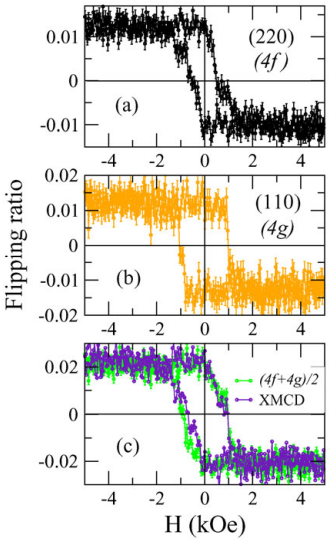


*FIG. 2. Element- and site-specific hysteresis loops for an applied field along the [001] easy axis at T = 300K. Top graph (a) shows (220) Bragg peak, E = 6.724 keV (b) (110) Bragg peak, E = 6.730 keV. Bottom graph (c) shows the average of the site-specific signals compared with the loop obtained in the absorption (XMCD) channel. The latter measures a weighted average of the two Nd sites.*

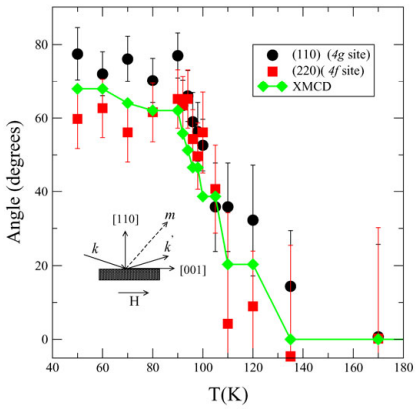


*FIG. 3. Site-specific SRT for inequivalent Nd sites. The angle between the in-scattering plane component of the magnetic moment and the [001] direction is retrieved from the measured decreases in charge-magnetic-interference integrated intensity by using the known polarization dependence of this scattering. The site-specific results are compared with the site-averaged angular deviation measured by XMCD.*

magnetic-interference signal to deviations in the magnetization direction in the 0° to 20° range. Despite this, the data suggest that the 4g sites may drive the SRT, since they start canting before the 4f sites. A competition between the MCAs at the inequivalent Nd sites has been proposed to be the driving force behind the SRT in this material [5]. Our results appear to indicate that such a competition might indeed occur in $Nd_2Fe_{14}B$.

## Acknowledgments

Use of the APS was supported by the U.S. Department of Energy, Office of Science, Office of Basic Energy Sciences, under Contract No. W-31-109-ENG-38.

## References

[1] G. Schutz et al., Phys. Rev. Lett. **58**, 737 (1987); J. Stohr et al., Surf. Rev. Lett. **5**, 1297 (1998).
[2] J. F. Herbst, Rev. Mod. Phys. **63**, 819 (1991).
[3] D. Sellmyer et al., Phys. Rev. Lett. **60**, 2077 (1988); S. Jaswal, Phys. Rev. B **41**, 9697 (1990).
[4] D. Haskel et al., IEEE Trans. Mag. (accepted, 2004); D. Haskel et al., Phys. Rev. Lett. **87**, 207201 (2001).
[5] D. Givord et al., Solid State Commun. **51**, 857 (1984).